Defence Research Establishment Pacific | Centre de recherches pour la défense pacifique | TECHNICAL MEMORANDUM 88-14

DEFENCE RESEARCH ESTABLISHMENT PACIFIC

CFB Esquimalt, FMO Victoria, B.C. V0S 1B0

MOTION MODEL FOR THE CORRECTION OF POINT-SOURCE DISTORTION IN RADIOGRAPHS OF HONEYCOMB

by

J. E. Boyd

September 1988

Approved by:

CHIEF

Research and Development Branch
Department of National Defence

Canada

91-00063/

ABSTRACT

One difficulty in the X-ray radiography of any object stems from the nature of the point source of radiation used. The point source dictates that the radiation passing through the object of interest is not parallel, consequently problems arise with honeycomb images. Radiation passing through the honeycomb parallel to the cell walls forms a clear and undistorted image of the structure, while other radiation forms a distorted image of the structure. The distortion is manifested as blurring of the cell walls and interpretation of the radiograph is made difficult. A numerical method is proposed which compensates for distortion in honeycomb radiography due to point-source radiation. The method is based on a model which assumes that the radiation source is parallel, and that the distortion is caused by motion during the integration of the radiograph. The result is that by treating the point-source distortion as motion blurring, the distortion can be corrected, within the constraints of the model.

TABLE OF CONTENTS

1. INTRODUCTION 1

2. MOTION MODEL FOR HONEYCOMB RADIOGRAPHS 2
   2.1. The Blurring Model 2
   2.2. Motion Model Deblurring 6

3. RESULTS 9

4. CONCLUSIONS 11

5. REFERENCES 12

1. INTRODUCTION

One difficulty in the X-ray radiography of any object stems from the nature of point-source radiation. The point source dictates that the radiation passing through the object of interest is not parallel. Often the non-parallel radiation is not problematic, such as the case when the thickness of the object is small compared to the distance between the source and the imaging plane (film or an intensifier in real-time systems). However, problems do arise from non-parallel radiation when honeycomb is radiographed. Radiation passing through the honeycomb parallel to cell walls forms a clear and undistorted image of the structure. Other radiation forms a distorted image of the structure. The distortion is manifested as blurring of the cell walls. Interpretation of the radiograph is made difficult for both man and machine, but short of altering the radiographic apparatus, the distortion is inevitable.

Digital image processing offers a solution. When the physical apparatus is constrictive, numerical methods may be used to compensate. This memorandum proposes a numerical method to compensate for distortion in honeycomb radiographs due to point-source radiation. The method is based on a model for the system which assumes that the radiation source is parallel, and that the distortion is caused by motion during the integration of the radiograph. Models for motion blurring are well understood, so a motion blur can be corrected. The result is that by treating the point-source distortion as motion blurring, the distortion can be corrected, within the constraints of the model.

Section 2 presents the theoretical basis of the motion model for point-source distortion in honeycomb, and the technique used to correct the distortion is outlined. Results from computer simulation and from actual radiographs are presented in Section 3. Based on these results, conclusions and recommendations for further work are stated in Section 4.

2. MOTION MODEL FOR HONEYCOMB RADIOGRAPHS

2.1. The Blurring Model

Figure 2.1 shows the apparatus for radiographing honeycomb with both parallel (ideal) and point sources. The motion model relates these two situations by making two assumptions. First, the honeycomb is uniform along the axis of the parallel radiation. Second, within a small region of the image the radiation from the point source is parallel. Based on these two assumptions the parallel and point-source radiation can be related as shown in Figure 2.2. Figure 2.2 shows graphically that the distortion due to the radiation passing through the honeycomb at an angle to cell walls is the same as if the radiation is parallel to the cell walls and the honeycomb is in motion during the integration of the image.

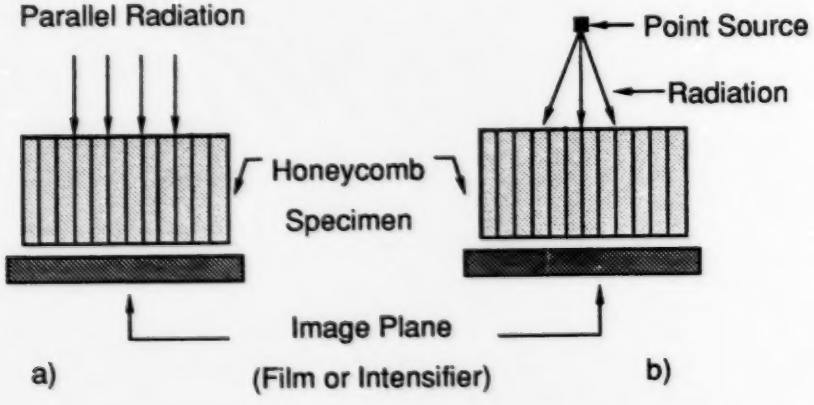

Figure 2.1: Apparatus for radiography of honeycomb, (a) parallel radiation (ideal), and (b) point-source radiation

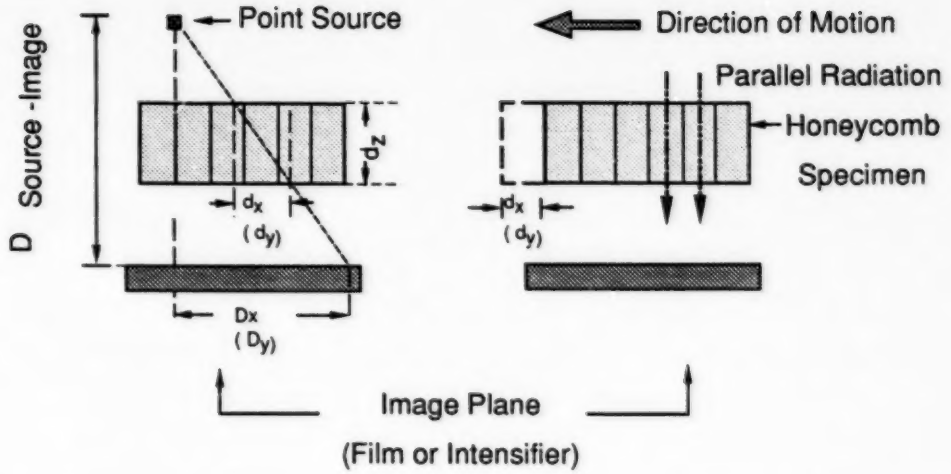

Figure 2.2: Motion model for point-source radiography of honeycomb.

In Figure 2.2 the image is in the x-y plane and the parallel radiation follows the z axis. Similar triangles are used to calculate d_x, the x axis motion, and d_y, the y axis motion. These are given by:

$$\frac{d_x}{d_z} = \frac{D_x}{D_{source\text{-}image}}, \tag{1}$$

$$d_x = \frac{D_x \; d_z}{D_{source\text{-}image}}, \tag{1a}$$

$$d_y = \frac{D_y \; d_z}{D_{source\text{-}image}}, \tag{1b}$$

where $D_{source\text{-}image}$ is the distance from the source to the image plane, d_z is the thickness of the honeycomb, and D_x and D_y are the x and y distances from the centre of the image to the point where the projection strikes the image plane. The ratio $d_z/D_{source\text{-}image}$ is the ratio of the honeycomb thickness to the distance from the source to the imaging plane. Both of

these quantities are measured in the same units so the ratio is dimensionless. If D_x is then measured in pixels the resulting value of d_x is a displacement in terms of the image pixels. An arbitrary image integration time, T, is assumed, which makes the x and y axis velocities:

$$v_x = \frac{d_x}{T} , \tag{2a}$$

$$v_y = \frac{d_y}{T} . \tag{2b}$$

Linear motion blurring based on these velocities can be modelled with the linear transfer function given by:

$$H_{motion}(u, v) = T \frac{\sin[\pi(u \cdot d_x + v \cdot d_y)]}{\pi(u \cdot d_x + v \cdot d_y)} e^{-j\pi(u \cdot d_x + v \cdot d_y)} , \tag{3}$$

where u and v are the spatial frequency variables corresponding to x and y. Since this transfer function is well known[1], its derivation is not shown here. Equation (3) may be expressed differently as:

$$H_{motion}(u,v) = T \cdot \mathrm{sinc}(\theta)\, e^{-j\theta}, \tag{4}$$

$$\text{where } \theta = \pi(u \cdot d_x + v \cdot d_y) .$$

The period, T, is assumed to be unity and can be ignored. Equation (4) can be considered as two terms, a magnitude term, $\mathrm{sinc}(\theta)$, and a phase term, $-\theta$. The magnitude term is identical to that of a rectangular low-pass filter which filters in the direction of the motion. It is the phase term, which is non-zero and asymetrical, that distinguishes the motion blur transfer function from a zero-phase low-pass filter.

Figure 2.3 shows examples of the motion model applied to synthetic honeycomb images. The image of an ideal honeycomb radiograph is in Figure 2.3(a). Figures 2.3(b) and 2.3(c) show the results of application of the motion model for two different thicknesses. To process the image it is first divided into square regions each measuring one sixteenth of the

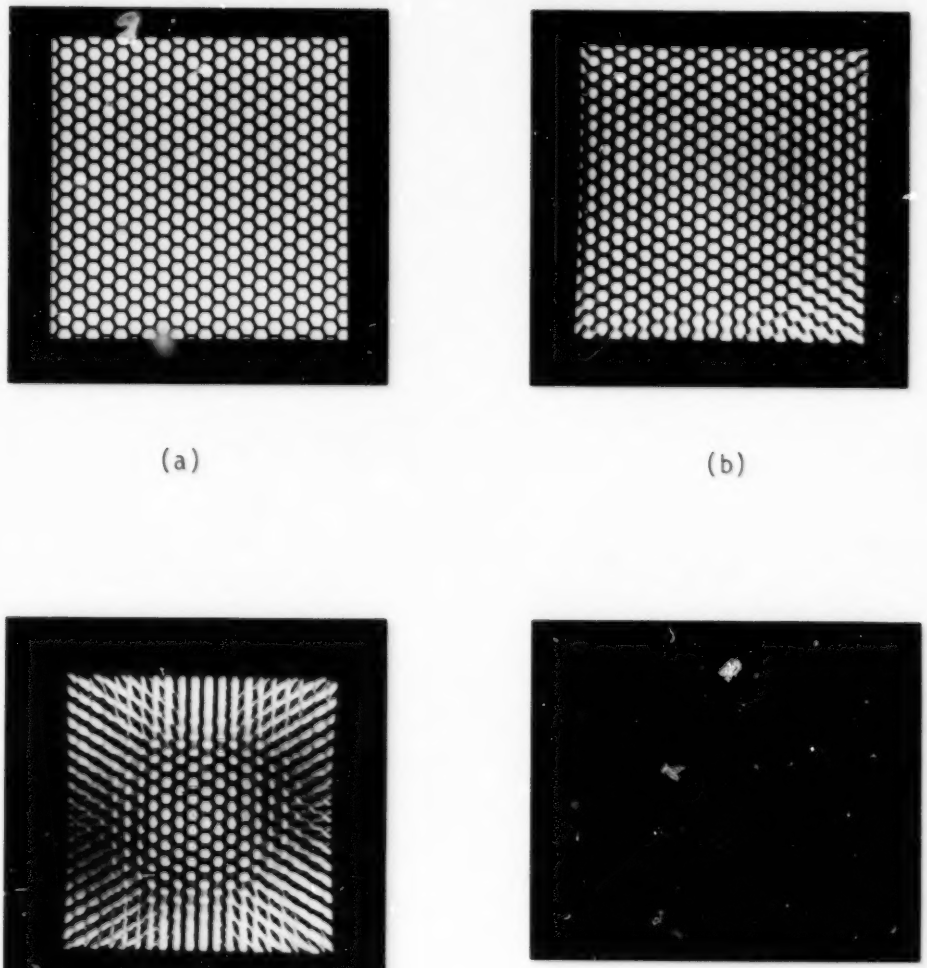

(a) (b)

(c) (d)

Figure 2.3: (a) simulated ideal honeycomb image, (b) simulated radiograph (d_z=0.05m, $D_{source-image}$=1.0m), (c) simulated radiograph (d_z=0.135m, $D_{source-image}$=1.0m), and (d) real radiograph (d_z=0.135m, $D_{source-image}$=1.0m).

full image size on each side. The squares are all processed separately using the displacements D_x and D_y as measured from the centre of the square to the centre of the image. The result is a convincing simulation of a honeycomb radiograph which supports the motion blur model of honeycomb radiographs. A genuine radiograph of thick honeycomb (d_z = 0.135m, $D_{source-image}$ = 1.0m) is shown in Figure 2.3(d) for comparison. Images in Figure 2.3 are all of resolution 256 by 256 pixels, with the exception of Figure 2.3(d) which has a resolution of 240 by 320 pixels. Section 2.2. deals with how the motion blur can be reversed to correct the radiograph.

2.2. Motion Model Deblurring

To correct for the point-source distortion the motion blurring process is reversed. Since the transfer function H_{motion} is known, the process is straight forward. The inverse transfer function, G_{motion} is given by:

$$G_{motion}(u,v) = \frac{1}{\text{sinc}(\theta)} e^{j\theta} . \qquad (5)$$

The transfer function in Equation (5) is not stable because the magnitude term, $1/\text{sinc}(\theta)$ goes to infinity when $\text{sinc}(\theta)$ is zero. However, as was stated in Section 2.1., the magnitude term is only a low-pass filter and the blur/deblur information is contained in the phase term. Therefore, the magnitude term may be ignored to give the new transfer function:

$$G_{motion}(u,v) = e^{j\theta} . \qquad (6)$$

Equation (6) is adequate to remove the motion blur, but the magnitude term of the blurring leaves the image low-pass filtered along the direction of

motion. To compensate for this the inverse transfer function is further modified to:

$$G_{motion}(u,v) = \text{sinc}(\phi)\, e^{j\theta}, \qquad (7)$$

$$\text{where } \phi = \pi(u \cdot d_y - v \cdot d_x) .$$

In words, Equation (7) compensates for the phase term by reversing the phase, and compensates for the magnitude term by filtering again with the same transfer function rotated by 90° and ignoring the phase. The output of the inverse transfer function is a phase corrected image which has been filtered by an isotropic low-pass filter.

Figure 2.4 shows an example of the motion deblurring process. The example is different from that of Figure 2.3 in that the motion blur is uniform across the entire image. Figure 2.4(a) shows the original image of an ideal honeycomb radiograph. The original image is blurred by a motion corresponding to $d_x = 10$ and $d_y = 10$ to produce the severely distorted image of Figure 2.4(b). Figure 2.4(c) shows the image after being corrected for phase only using Equation(6). A better corrected image is shown in Figure 2.4(d) were the motion blur is corrected for both phase and magnitude by Equation (7). Images in Figure 2.4 are all of resolution 128 by 128 pixels. This image provides a clear view of the honeycomb cells with a small loss of definition due to the low-pass filtering.

Section 3. augments these examples with examples taken from real honeycomb data.

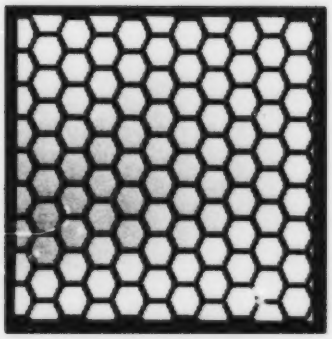

(a)

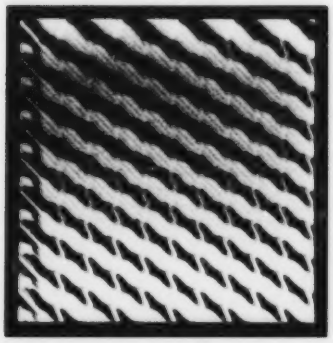

(b)

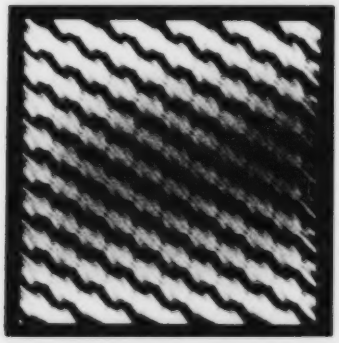

(c)

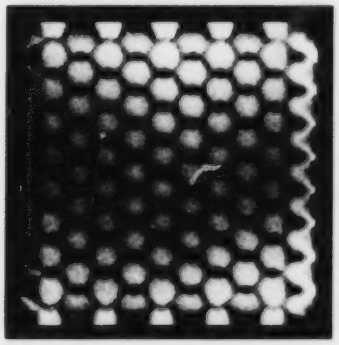

(d)

Figure 2.4: (a) simulated ideal honeycomb image, (b) blurred image (d_x=10, d_y=10), (c) image deblurred using Equation (6), and (d) image deblurred using Eqation (7).

3. RESULTS

Reproduction of the simulation results of Section 2 with real data is difficult. The two assumptions made are not exactly true when working with real apparatus. It is no longer true that the honeycomb is uniform along the z axis. Also, blurring is not exactly uniform in a small region of the image. However, it is possible to obtain data which are close to meeting the assumptions, and motion deblurring is effective.

Figure 3.1(a) shows a honeycomb radiograph (from a real-time system) which nearly meets the assumptions. The honeycomb has no face sheets attached to it so within certain tolerances it is uniform, parallel to the cell walls. The radiograph is of a small enough region that the distortion is nearly uniform throughout the image. d_x and d_y are measured from the radiograph and the radiograph is corrected using Equation (7). The resulting image is shown in Figure 3.1(b). The effect of non-uniform distortion is clear in Figure 3.1(b). The centre of the image shows well restored honeycomb cells while cells on the right or the left of the image remain partially distorted. Regardless, the corrected image is clearer and more easily interpreted, both manually and automatically. Images in Figure 3.1 are 128 by 128 pixels.

A honeycomb radiograph from film is shown in Figure 3.2(a). The honeycomb in this example is from the horizontal stabilator of a CF-18. Adhesive which bonds graphite/epoxy face sheets to the honeycomb is visible. It is the presence of this adhesive which violates the assumption of uniformity along the z axis and confounds the data. The effect is evident in Figure 3.2(b) which shows the corrected image. The image is cluttered and difficult to interpret. Images in Figure 3.2 are 128 by 128 pixels.

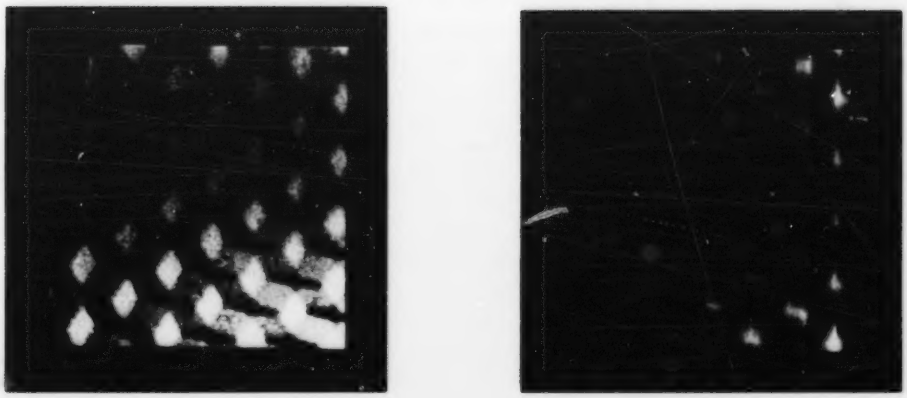

(a) (b)

Figure 3.1: (a) real - time radiograph of honeycomb, and (b) deblurred image.

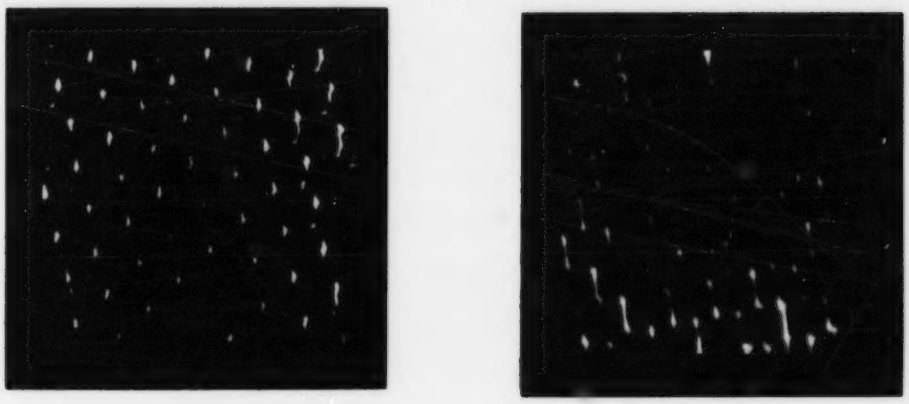

(a) (b)

Figure 3.2: (a) film radiograph of honeycomb, and (b) deblurred image.

4. CONCLUSIONS

It has been shown that motion blurring can be used to successfully model the distortion of honeycomb radiographs resulting from the use of a point source. Also, application of the inverse of the model can be used to numerically correct honeycomb radiographs for this distortion.

The model assumes that the honeycomb is uniform parallel to its cell walls and that the point-source distortion is uniform in small regions of the radiograph. These assumptions are important because they can be difficult to meet for real data. In cases where the assumptions can be met, the method produces images that are corrected for the distortion. Where the assumptions cannot be met, the corrected images are difficult to interpret.

Future work should be directed toward dealing with situations where the assumptions cannot be met, in particular, the assumption of uniformity parallel to cell walls. In aircraft structures where the honeycomb is bonded to face sheets, the presence of face sheets and adhesives confound the data. The aircraft structures cannot be changed so it is necessary that the numerical correction be improved. The problem of non-uniform distortion can be handled by ensuring that a sufficiently small region of the radiograph is used.

So far defects in the honeycomb have not been considered. In the context of the model, defects are violations of the z axis uniformity requirement. When a defect is present, the deblurring process will distort it. However, the defect will still be visible, and the integrity of automatic and manual inspection will not be affected.

With some improvement the motion blur correction for point-source distortion offers the ability to numerically compensates for some long-standing problems in the radiography of honeycomb structure.

5. REFERENCES

1. R.C. Gonzales, P. Wintz, Digital Image Processing, Addison-Wesley, 1977, pp 201-207.

DISTRIBUTION

REPORT NUMBER:	DREP Technical Memorandum 88-14
TITLE:	Motion Model for the Correction of Point-Source Distortion in Radiographs of Honeycomb
AUTHORS:	J.E. Boyd
DATED:	September 1988
SECURITY GRADING:	UNCLASSIFIED

1 - DSIS

1 - CRAD
1 - DGRD Ops
1 - DRDA
1 - DRDL
1 - DRDM

1 - DGAEM
2 - DFTEM
2 - DAS Eng

1 - AMDU

8 - DREP

DOCUMENT CONTROL DATA

(Security classification of title, body of abstract and indexing annotation must be entered when the overall document is classified)

1. ORIGINATOR (the name and address of the organization preparing the document. Organizations for whom the document was prepared, e.g. Establishment sponsoring a contractor's report, or tasking agency, are entered in section 8.)

Defence Research Establishment Pacific
FMO Victoria, BC
V0S 1B0

2. SECURITY CLASSIFICATION (overall security classification of the document. including special warning terms if applicable)

UNCLASSIFIED

3. TITLE (the complete document title as indicated on the title page. Its classification should be indicated by the appropriate abbreviation (S,C,R or U) in parentheses after the title.)

Motion Model for the Correction of Point-Source Distortion in Radiographs of Honeycomb (U)

4. AUTHORS (Last name, first name, middle initial)

Boyd, J. E.

5. DATE OF PUBLICATION (month and year of publication of document)

6a. NO. OF PAGES (total containing information. Include Annexes, Appendices, etc.)

17

6b. NO. OF REFS (total cited in document)

1

7. DESCRIPTIVE NOTES (the category of the document, e.g. technical report, technical note or memorandum. If appropriate, enter the type of report, e.g. interim, progress, summary, annual or final. Give the inclusive dates when a specific reporting period is covered.)

DREP Technical Memorandum 88-14

8. SPONSORING ACTIVITY (the name of the department project office or laboratory sponsoring the research and development. Include the address.)

DREP

9a. PROJECT OR GRANT NO. (if appropriate, the applicable research and development project or grant number under which the document was written. Please specify whether project or grant)

26B

9b. CONTRACT NO. (if appropriate, the applicable number under which the document was written)

10a. ORIGINATOR'S DOCUMENT NUMBER (the official document number by which the document is identified by the originating activity. This number must be unique to this document.)

DREP TM 88-14

10b. OTHER DOCUMENT NOS. (Any other numbers which may be assigned this document either by the originator or by the sponsor)

11. DOCUMENT AVAILABILITY (any limitations on further dissemination of the document, other than those imposed by security classification)

(X) Unlimited distribution
( ) Distribution limited to defence departments and defence contractors; further distribution only as approved
( ) Distribution limited to defence departments and Canadian defence contractors; further distribution only as approved
( ) Distribution limited to government departments and agencies; further distribution only as approved
( ) Distribution limited to defence departments; further distribution only as approved
( ) Other (please specify):

12. DOCUMENT ANNOUNCEMENT (any limitation to the bibliographic announcement of this document. This will normally correspond to the Document Availabilty (11). However, where further distribution (beyond the audience specified in 11) is possible, a wider announcement audience may be selected.)

13. ABSTRACT (a brief and factual summary of the document. It may also appear elsewhere in the body of the document itself. It is highly desirable that the abstract of classified documents be unclassified. Each paragraph of the abstract shall begin with an indication of the security classification of the information in the paragraph (unless the document itself is unclassified) represented as (S), (C), (R), or (U). It is not necessary to include here abstracts in both offical languages unless the text is bilingual).

One difficulty in the X-ray radiography of any object stems from the nature of the point source of radiation used. The point source dictates that the radiation passing through the object of interest is not parallel, consequently problems arise with honeycomb images. Radiation passing through the honeycomb parallel to the cell walls forms a clear and undistorted image of the structure, while other radiation forms a distorted image of the structure. The distortion is manifested as blurring of the cell walls and interpretation of the radiograph is made difficult. A numerical method is proposed which compensates for distortion in honeycomb radiography due to point-source radiation. The method is based on a model which assumes that the radiation source is parallel, and that the distortion is caused by motion during the integration of the radiograph. The result is that by treating the point-source distortion as motion blurring, the distortion can be corrected, within the constraints of the model.

14. KEYWORDS, DESCRIPTORS or IDENTIFIERS (technically meaningful terms or short phrases that characterize a document and could be helpful in cataloguing the document. They should be selected so that no security classification is required. Identifiers, such as equipment model designation, trade name, military project code name, geographic location may also be included. If possible keywords should be selected from a published thesaurus. e.g. Thesaurus of Engineering and Scientific Terms (TEST) and that thesaurus-identified. If it is not possible to select indexing terms which are Unclassified, the classification of each should be indicated as with the title.)

radiography

honeycomb

distortion

image processing

convolution